Journal of Polish CIMAC
Gdansk University of Technology
The Faculty of Ocean Engineering and Ship Technology

NUMERICAL AND EXPERIMENTAL STUDY ON ALUMINIUM PIPE BENDING PROCESS

Piotr Domanowski[*], Bartosz Nowak[**]

[*] *University of Technology and Life Sciences in Bydgodszcz*
al. Prof. S. Kaliskiego 7, 85-789 Bydgoszcz, Poland
e-mail: piotr.domanowski@utp.edu.pl

[**] *Kazimierz Wielki University in Bydgoszcz*
ul. Chodkiewicza 30, 85-064 Bydgoszcz, Poland

Abstract

In this paper the analysis of cold working bending process of the aluminum pipe was presented based on both numerical simulations and experimental tests. The parameters such as wall thickness above and below bending axis were compared and discussed for both numerical simulations and experimental tests. The numerical simulations were performed in Abaqus 6.9/CAE computational environment on the basis of finite element method while the bending machine was designed and constructed for the purpose of tests. The usefulness of numerical simulations was also discussed.

Keywords: *bending process, numerical simulations*

1. Introduction

Bending is a process in which metal can be deformed by plastic deformation. This results in changes in both its dimension and its shape. In the bending process material is stressed beyond the yield strength but below the ultimate tensile strength [2, 7]. Bending process is performed on machines called benders.

The aim of this study was to perform the analysis of the bending process on the basis of numerical simulations and of technological process. The study was focused on the changes of cross-sectional dimensions of the pipe which took place during the process.

To fulfilled the aim of the study experimental tests conducted on bending machine in technological process were performed as well as the numerical simulations of the bending process.

The outcomes and the conclusions presented in this paper were used in improving of the design of the automatic bending machine constructed for the purpose of the service in industry [6].

2. Materials and methods

The object of the analysis was the pipe made out of aluminum type WA6060. The pipe belongs to the fuel supply system of the car produced in Poland. The initial diameter of the pipe was 8 mm and initial wall thickness 1 mm. The pipe is bent during bending process. The final shape and dimensions of the bent pipe are shown in Fig. 1.

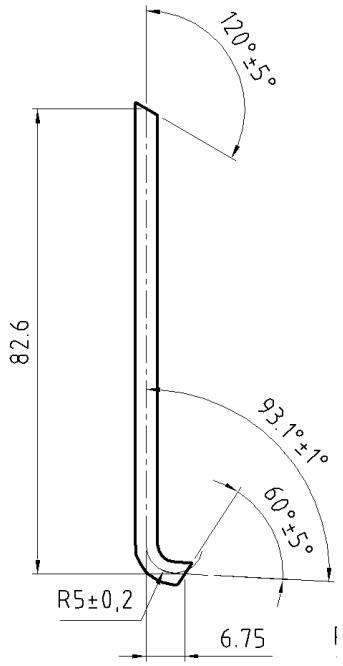

Fig. 1. The main dimensions of the pipe

The material of the pipe consists of aluminum and other additives such as magnesium, silicone and iron. This type of aluminum alloy was designated as EN WA 6060. Material properties of aluminum alloy WA 6060 are presented in Tab. 1. The properties of aluminum alloy were based on literature investigations [4-7] and data given by the producer of pipes. The main material's features includes good strength for tensile stresses and moderate fatigue strength. The material possesses high ability to forming profiles with complicated shapes.

Tab. 1. Mechanical properties of aluminum alloy WA 6060

Property	Symbol	Value
Young modulus	E	70GPa
Poisson's ratio	v	0.30
Yield strength	R_{p02}	160MPa
Ultimate tensile strength	R_m	190MPa
Elongation	A	0.16

The process of pipe bending is performed in room temperature. The pipe is wrapped around the rotating roller. The geometry of the roller (rotating bending die) is presented in Fig. 2.

Numerical calculations were performed in computational environment Abaqus/CAE 6.9 with the use of finite element method. The graphical preprocessor of that environment was used for

preparation of geometry of numerical model. Processor of computational environment was used to perform calculations based on Newton-Rawson procedure [3, 8]. The results of performed calculations were gathered and presented with use of post-processor of Abaqus/CAE 6.9 computational environment.

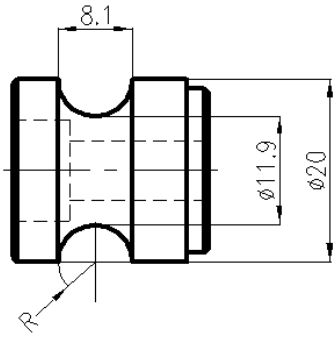

Fig. 2. The main dimensions of the roller

The geometry of the numerical model of the pipe consisted of: pipe, upper holder of bending head, lower holder of bending head integrated with rotational die, upper holder of the feeding head and lower holder of the feeding head. The geometry and the orientation of the elements mentioned above are presented in Fig. 3.

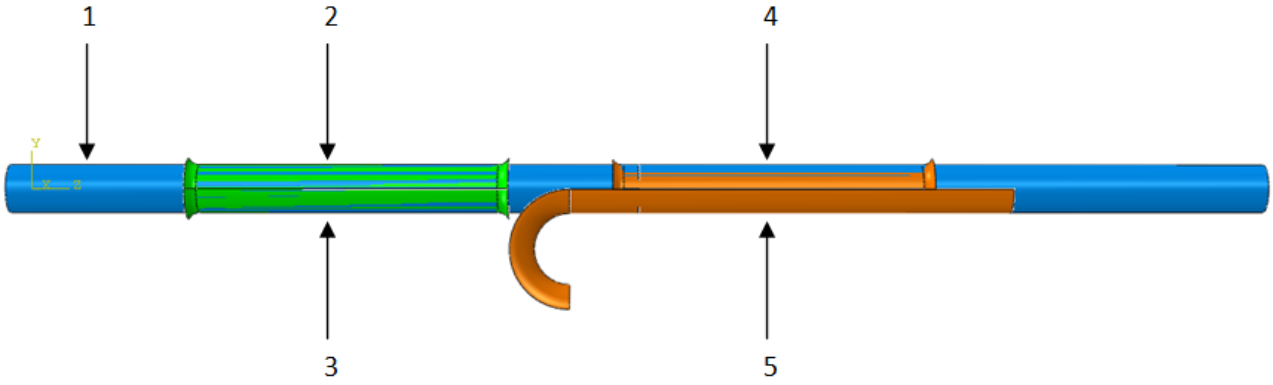

Fig. 3. Geometry of numerical model; 1- pipe, 2- upper holder of the feeding head, 3 - lower holder of the feeding head, 4 - upper holder of the bending head, 5 - lower holder of the bending head integrated with rotational die

Nonlinear model of aluminum material was used in calculations. Properties of aluminum material WA 6060 supplied by the producer were mentioned in the previous section of the text. Modeling of aluminum material was based on linear elastic-plastic model of material with linear hardening elaborated on the basis Tab. 1. Isotropic hardening was defined on the basis of yield stress and yield strain. Material that was taken into account was isotropic and homogenous. The characteristics of stress-strain relations for simplified aluminum material model based on technical data delivered by producer of material and full stress-strain relation in extension test are presented in Fig. 4.

In the numerical analysis the contact between the following surfaces was defined: upper holder of the feeding head - pipe, lower holder of the feeding head - pipe, upper holder of the bending head - pipe, lower holder of the bending head integrated with rotational die - pipe. In numerical procedure the value of static friction coefficient was $\mu s = 0.2$ and kinematic friction coefficient $\mu k = 0{,}05$. The following boundary conditions were applied to the numerical model:

upper holder of the bending head - full fixation (all degrees of freedom restrained) only rotations in Y-Z plane allowed, lower holder of the bending head integrated with rotational die - full fixation (all degrees of freedom restrained) only rotations in Y-Z plane allowed, upper holder of the feeding head - rectilinear movement along Z axis with the velocity equaled to angular velocity of roller, lower holder of the feeding head - full fixation (all degrees of freedom restrained).

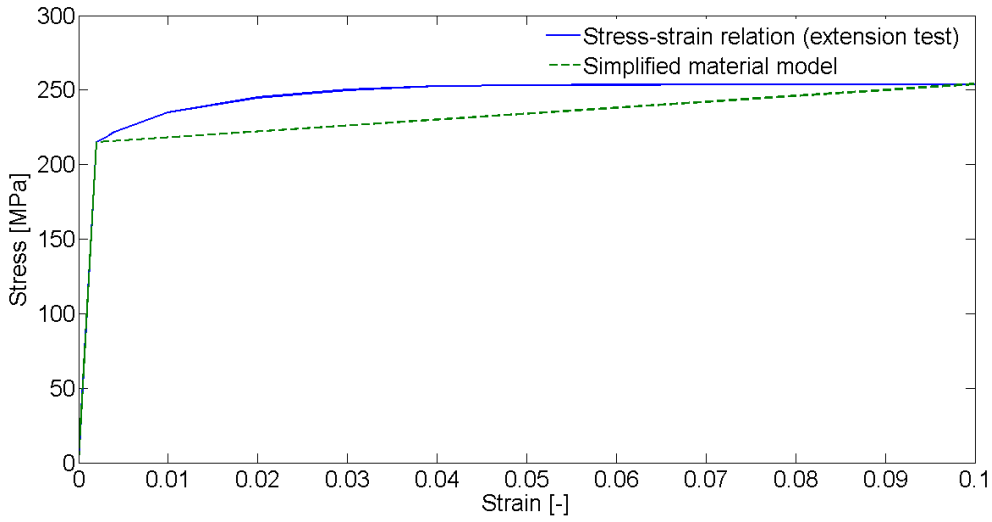

Fig. 4. Characteristics of stress-strain relations

Rotation was realized by revolution of lower holder of bending head integrated with rotational die and upper holder of the bending head by angle 90°. Translations and rotations are shown in Fig. 5. Boundary conditions and kinematics of used in numerical simulations were similar to those in experimental tests.

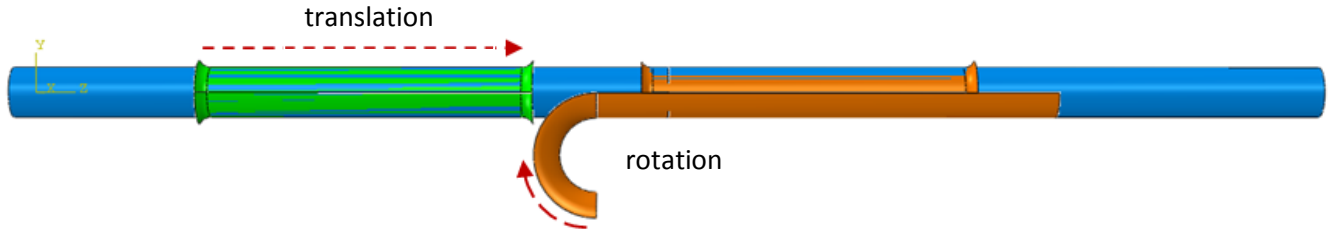

Fig. 5. View and description of boundary conditions

Discretization of the pipe with the use of finite element method was performed by use of continuum hexahedral finite elements with linear shape function. Eight nodes were located in the corners of each element. Each node had three translational degrees of freedom. The finite elements were labeled according to [1] as C3D8R. The number of finite elements equalled for pipe was 8388. Discretization of the upper holder of bending head, lower holder of bending head integrated with rotational die, upper holder of the feeding head and lower holder of the feeding head was done by use of rigid non-deformable shell finite elements. Those finite elements were labeled according to [1] as R3D4. The number of finite elements was as follows: the upper holder of bending head 1560, lower holder of bending head integrated with rotational die 1896, upper holder of the feeding head 1560 and lower holder of the feeding head 1560.

The total number of finite elements was 15 650, while total number of nodes was 21 209. Due to symmetry of the numerical model only half of the model was taken into account.

The view of mesh of the pipe and holders are presented in Fig. 6.

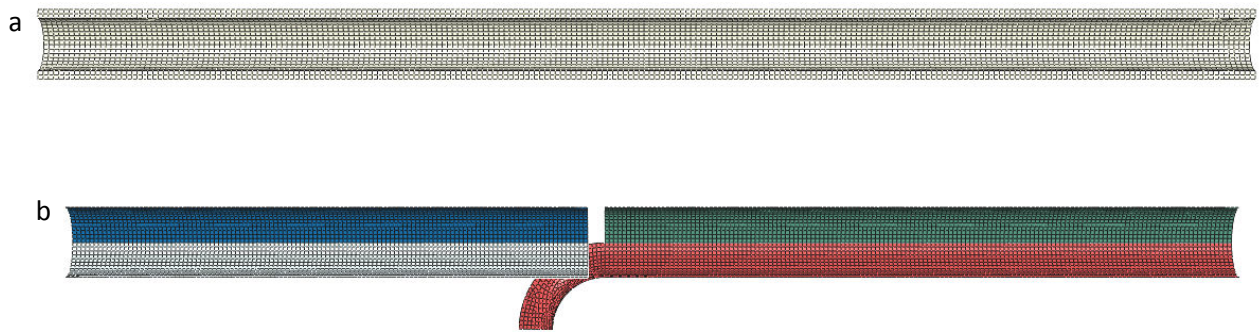

Fig. 6. Finite element mesh; a - pipe, b - holders (tools)

In numerical simulations the problem was described by the following equation: (1):

$$\mathbf{M}\ddot{\mathbf{u}} + \mathbf{C}\dot{\mathbf{u}} + \mathbf{K}\mathbf{u} = \mathbf{P} \tag{1}$$

where:

$\mathbf{M}$ – mass matrix,

$\mathbf{C}$– damping matrix,

$\mathbf{K}$ – stiffness matrix,

$\mathbf{P}$ – vector of external forces,

$\mathbf{u}$ – vector of nodal displacements,

$\dot{\mathbf{u}}$-– vector of nodal velocities,

$\ddot{\mathbf{u}}$– vector of nodal accelerations.

Direct integration method was used for solving equation:

$$\dot{u}^{N}_{\left(i+\frac{1}{2}\right)} = \dot{u}^{N}_{\left(i-\frac{1}{2}\right)} + \frac{\Delta t_{(i+1)} + \Delta t_{(i)}}{2}\ddot{u}^{N}_{(i)} \tag{2}$$

$$u^{N}_{(i+1)} = \dot{u}^{N}_{(i)} + +\Delta t_{(i+1)}\dot{u}^{N}_{\left(i+\frac{1}{2}\right)} \tag{3}$$

where:

i – iteration,

N – degree of freedom.

The machine for automatic pipe bending was constructed for purpose of realising the bending process. It consists of the following devices: material feeder, bender (bending device), unit of semi-finished products and unit of finished products. Scheme of the bending device is presented in Fig. 7. The bending device consists of: upper holder of the feeding head, lower holder of the feeding head, upper holder of the bending head, lower holder of the bending head integrated with rotational die.

The upper holder of the feeding head is connected to force actuator equipped with adjustable pressure force in range 0 - 300 N. The machine is equipped with feeder of the material which includes holder and force actuator. The machine is designed for running in automatic cycle. The elements responsible for automatization of the process are not shown in Fig. 7. Pneumatic actuators and servo-motors were used in engineering of power transmission. Power drive of rotation holder was realized by motoreducer, which consists of servo-motor and planetary gear with velocity ratio of 1:100. The planetary gear used in construction of the power drive of rotation holder had circumferential backlash smaller than 5'.

The bending process is realized on the bending machine in the following way. The pipe is loaded to bender device from semi-finished products unit and secured firmly in pneumatic holders. The pressure force of the holders is set to ensure the secure fixation of the pipe. Then the rotation pneumatic holder rotates about the angle of 90° and makes the pipe to be bent. When the bending is finished rotation pneumatic holder rotates back about the angle of 90°and the pipe is pushed forward to the jaw of the saw. The desired length of bent pipe is cut. After that process starts again.

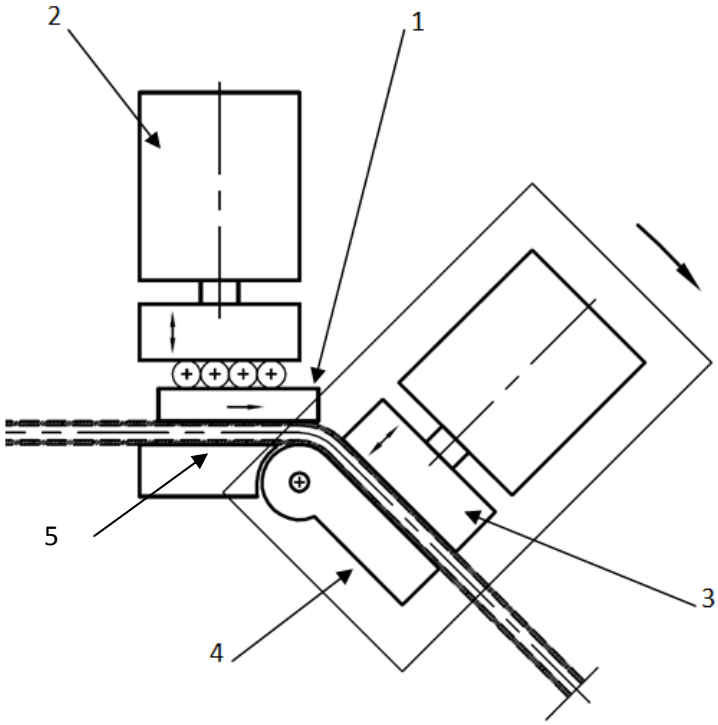

Fig. 7. Scheme of the bending device; 1- upper holder of the feeding head, 2 - lower holder of the feeding head, 3 - upper holder of the bending head, 4 - lower holder of the bending head integrated with rotational die, 5 - pressure force actuator

3. Results and discussion

The results consist of outcomes obtained on the basis of numerical simulations and experimental tests. They include: pipe's diameter measured in the bending plane, thickness of the pipe's wall above bending axis and thickness of the pipe's wall below bending axis. Measurements were done on selected fragment of the pipe, which is shown in Fig. 8. It represents wrapped

around the roller die fragment of the pipe in range 0° - 90°. The measurements were performed every 5°.

The results of numerical simulations were obtained with use of pre-processor of Abaqus/CAE computational environment. Measurements in experimental tests were conducted on the basis of computer aided measurements of pipe's micro- section. The scheme for experimental measurements of pipe's parameters after bending process is presented in Fig. 9.

The cross-section of the pipe with the distribution of pipe's thickness wall and the magnitude of equivalent plastic strains were presented in Fig. 10 while cross-section of the pipe for experimental tests in Fig. 11.

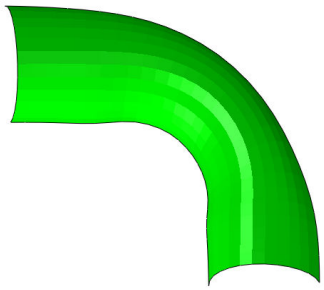

Fig. 8. The measuring length of the pipe after deformation

In discussion the results obtained from numerical simulations and experimental tests have been compared. It can be observed that during bending process the cross-sectional area of bending material was changed. It was caused by changing of transversal dimensions of compressed and tensioned layers of the material. The differences between numerical and experimental results were in range 1% - 26% for all parameters on the measuring length.

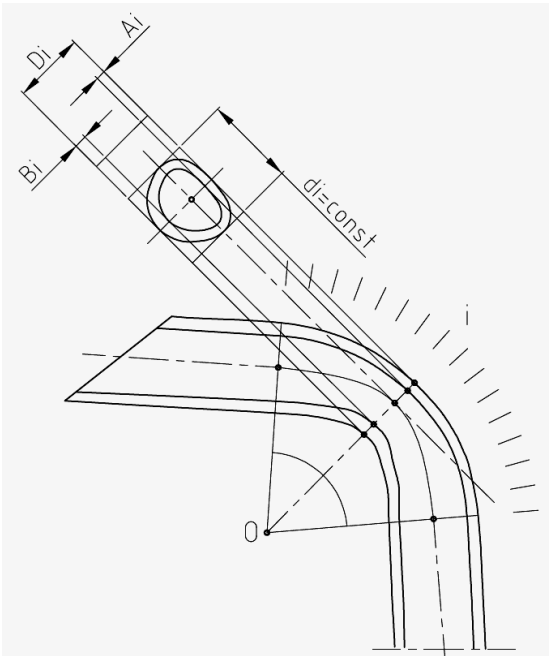

Fig. 9. Measuring of pipe's thickness

The comparison of distribution of the pipe's diameter on the measuring length of the pipe for numerical simulations and experimental tests was shown in Fig. 12. It can be noticed that the pipe's diameter decreases in the plane of bending. The smallest value obtained in numerical simulations was 5.11 mm while in experimental tests was 5.92 mm. The difference between these values results 16 %. It must be stated that the position of the smallest value in experimental tests is shifted by 1° comparing to numerical simulations. However experimental and numerical results are in good qualitative agreement.

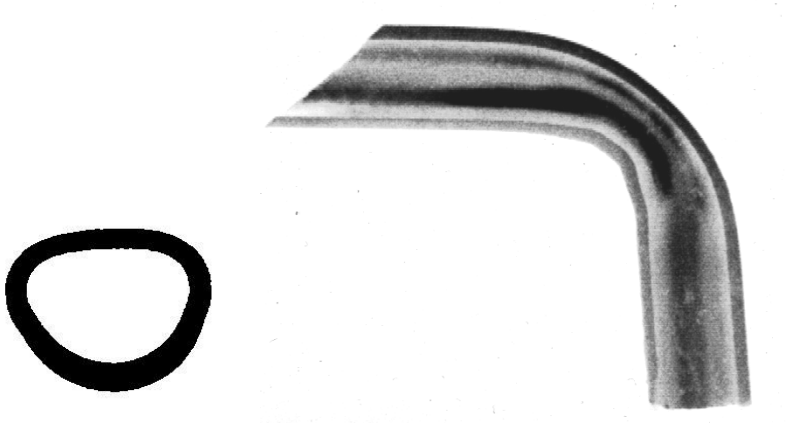

Fig. 10. Section of the pipe - experimental test

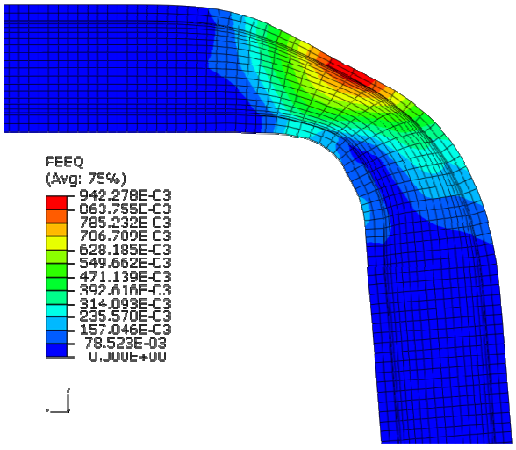

Fig. 11. Distribution of pipe's thickness wall and the magnitude of equivalent plastic strains

The comparison of distribution of the pipe's thickness above the bending axis on the measuring length of the pipe for numerical simulations and experimental tests was shown in Fig. 13. The smallest value obtained in numerical simulations was 0,56 mm while in experimental tests was 0.71 mm. The difference between these values results 26 %. It must be stated that the position of the smallest value in experimental tests is shifted by 2° comparing to numerical simulations. However experimental and numerical results are in good qualitative agreement.

The comparison of distribution of the pipe's thickness below the bending axis on the measuring length of the pipe for numerical simulations and experimental tests was shown in

Fig. 14. The smallest value obtained in numerical simulations was 0,84 mm while in experimental tests was 0.98 mm. The difference between these values results 17 %. It must be stated that the position of the smallest value in experimental tests is shifted by 5° comparing to numerical simulations. However experimental and numerical results are in good qualitative agreement.

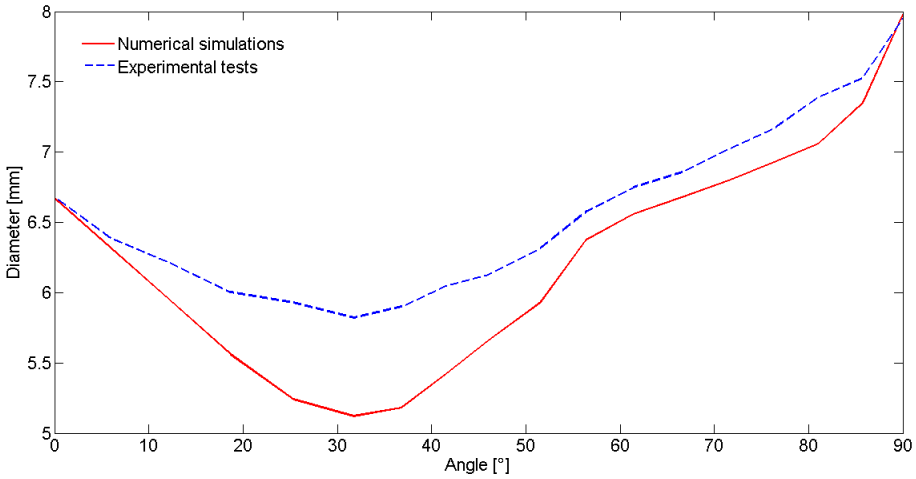

Fig. 12. The comparison of distribution of pipe's diameter on measuring length for experimental and numerical results

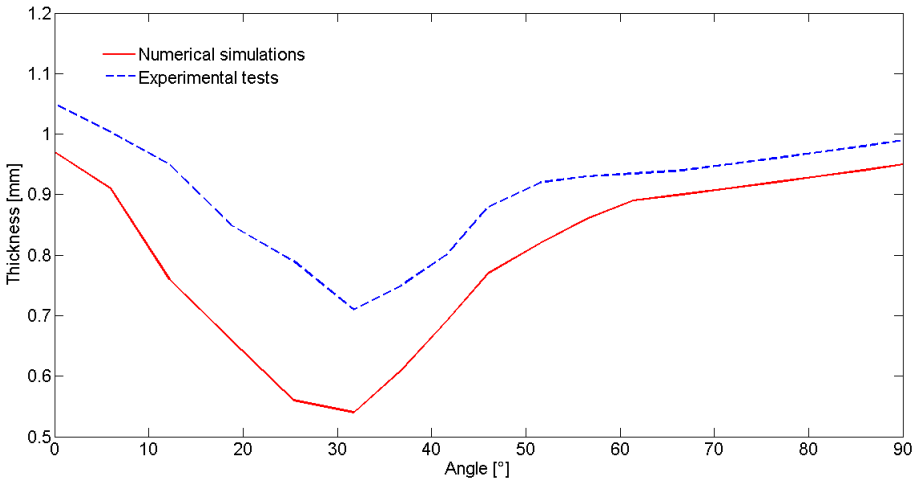

Fig. 13. The comparison of distribution of pipe's thickness above neutral axis of bending on measuring length for experimental and numerical results

4. Conclusions

It can be seen from the analysis presented above that the results of computer simulations and experimental tests are in good qualitative agreement, even though application of simplified material model in numerical analysis. In some cases the values of numerical and experimental results were different. This discrepancy could be caused by application of aluminum material model which was based on linear elastic-plastic model with linear hardening, which in fact was a significant simplification. However the technical data of the material supplied by the producer

often includes only parameters such as Young modulus, Poisson ratio, Yield stress, Ultimate stress which are not sufficient to obtain full stress-strain relation.

Results improvements could be obtain by application of more sophisticated model of the material.

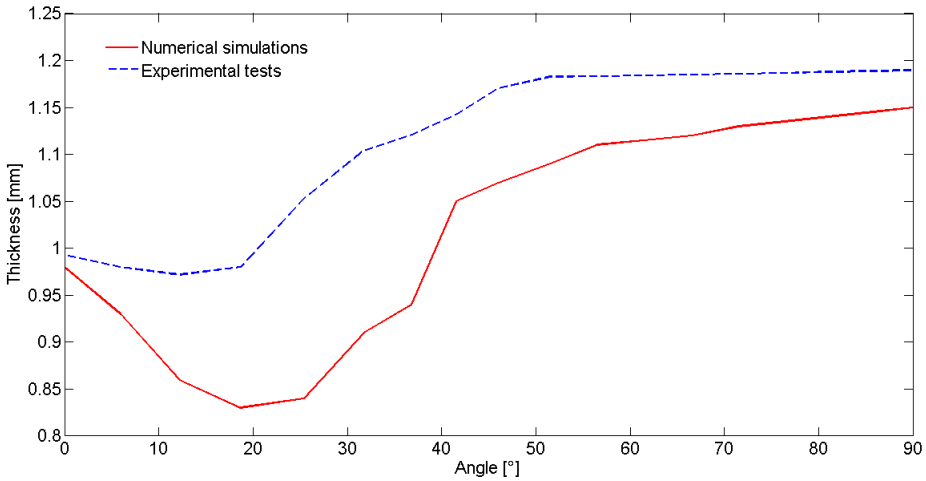

Fig. 14. The comparison of distribution of pipe's thickness below neutral axis of bending on measuring length for experimental and numerical results

References

[1] ABAQUS. *Abaqus manuals*. Inc. Providence, 2005.
[2] Altan T, *Metal forming handbook*. Springer Verlag Berlin Heidelberg, 1998.
[3] Bathe K. *Finite Element Procedures*. Prentice Hall, 1996.
[4] Boyer H E. *Atlas of strain-stress curves*. ASM International, 1987.
[5] Dixit U M, Dixit U S. *Modeling of metal forming and machining processes by finite element and soft computing methods*. Springer Verlag London, 2006.
[6] Domanowski P, Wocianiec R. *Structure Design and Numerical Control System of Automatic Pipe Bending Machine,* 13th International Conference on Developments in Machinery Design and Control, Bydgoszcz, Poland 2009.
[7] Wogoner R. H, Chenot U. S. *Fundamentals of metal forming,* Wiley, 1996.
[8] Zienkiewicz O. C., Taylor R. L. *The Finite Element Method Vol. 1*. Butterworth-Heinemann, 2000.